Relevance Of Artificial Roughness To Enhance Heat Transfer In Solar Air Heater - A Review

Rewaram Verma[1] and Dr. K R. Aharwal[2]

[1] *Scholar Mewar University Gangrar Chittorgarh- India, Shri Venkteshwar Institute of Technology, Indore -India*

[2] *Department of Mechanical Engineering, Maulana Azad National Institute of Technology , Bhopal -India*

Abstract- Improvement in the thermo hydraulic performance of a solar air heater can be done by enhancing the heat transfer. In general, heat transfer enhancement techniques are divided into two groups: active and passive techniques. Providing an artificial roughness on a heat transferring surface is an effective passive heat transfer technique to enhance the rate of heat transfer to fluid flow. In this paper, reviews of various artificial roughness elements used as passive heat transfer techniques, in order to improve thermo hydraulic performance of a solar air heater, with little penalty of friction and Correlations developed by various researchers with the help of experimental results for heat transfer and friction factor for solar air heater ducts by taking different roughened surfaces geometries are given in tabular form. These correlations are used to predict the thermo hydraulic performance of solar air heaters having roughened ducts. The objective is to provide a detailed review on heat transfer enhancement by using an artificial roughness technique. This paper will be very helpful for the researchers who are researching new artificial roughness for solar air heater ducts to enhance the heat transfer rate and comparing with artificial roughness already studied by various researchers.

Keywords: solar air heater, artificial roughness, active & passive technique, heat transfer, friction factor

Introduction -The rapid depletion of fossil fuel resources has necessitated an urgent search for alternative sources of energy. of the many alternatives, solar energy stands out as the brightest long range promise towards meeting the continually increasing demand for energy. Solar energy is available freely and an indigenous source of energy provides a clean and pollution free atmosphere. The simplest and the most efficient way to utilize solar energy is to convert it into thermal energy for heating applications by using solar collectors. Solar air heaters, because of their inherent simplicity are cheap and most widely used collector devices. Solar air heaters are being used for many applications at low and moderate temperatures. Some of these are crop drying, timber seasoning, space heating, chicken brooding and curing / drying of concrete/clay building components. The thermal efficiency of solar air heaters is low due to two reasons: low thermal capacity of air and a low heat transfer co-efficient between the absorber plate and air flow through duct. In order to make the solar air heater economically more viable, their thermal efficiency needs to be improved. This can be done by enhancing the heat transfer co-efficient between the

absorber plate and air flow through a duct. In general, heat transfer co-efficient enhancement techniques can be divided into two groups; namely active and passive. The active techniques require external forces, e.g. electric field, acoustic and surface vibration. The passive techniques require special surface geometries, Passive techniques have being used by researchers for 140 years for increasing the heat transfer rate in a heat exchanger.

Concept of artificial roughness

Artificial roughness is basically a passive heat transfer enhancement technique by which thermo hydraulic performance of a solar air heater can be improved. The artificial roughness has been used extensively for the enhancement of forced convective heat transfer, which further requires flow at the heat-transferring surface to be turbulent. However, energy for creating such turbulence has to come from the fan or blower and the excessive power is required to flow air through the duct. Therefore, it is desirable that the turbulence must be created only in the region very close to the heat transferring surface, so that the power requirement may be lessened. This can be done by keeping the height of the roughness elements to be small in comparison with the duct dimensions.

The key dimensionless geometrical parameters that are used to characterize roughness are:

1. Relative roughness pitch (p/e): Relative roughness pitch (p/e) is defined as the ratio of distance between two consecutive ribs and height of the rib.

2. Relative roughness height (e/D): Relative roughness height (e/D) is the ratio of rib height to equivalent diameter of the air passage.

3. Angle of attack (_): Angle of attack is inclination of rib with direction of air flow in duct.

4. Shape of roughness element: The roughness elements can be two-dimensional ribs or three-dimensional discrete elements, transverse or inclined ribs or V-shaped continuous or broken ribs with or without gap. The roughness elements can also be arc-shaped wire or dimple or cavity or compound rib-grooved. The common shape of ribs is square but different shapes like circular, semi-circular and chamfered have also been considered to investigate thermo hydraulic performance.

5. Aspect ratio: It is ratio of duct width to duct height. This factor also plays a very crucial role in investigating thermo-hydraulic performance.

Researcher has been taken some geometry to investigate the effect of thermal performance of air heater.

V- Shaped rib-[1] Muluwork et al. have investigated the effect of a staggered discrete V- apex up and down on the thermal performance as depicted in Figure 4 The Stanton number for V-down discrete ribs was higher than the corresponding V-up and transverse discrete roughened surfaces. The Stanton number ratio enhancement was found to be 1.32 to 2.47 in the range of parameters covered in the investigation.

Further for the Stanton number, it was seen that the ribbed surface friction factor for V-down discrete ribs was highest among the three configurations investigated. [2] Momin et al. has investigated the effect of relative roughness height and angle of attack for a fixed relative roughness pitch of 10 with the Reynolds number range of 2500 to 18000 for a V-shaped rib as depicted in Figure 5. It was found that the rate of increase of the Nusselt number with an increase in Reynolds number is lower than the rate of increase of the friction factor. It was found that for the relative roughness height of 0.034, the V-shaped ribs enhanced the values of Nusselt number by 1.14 and 2.30 times over inclined ribs and smooth plate. [3] Karwa et al. has investigated and revealed the effect of transverse, inclined, V-continuous and V-discrete patterns on heat transfer and the friction factor in a rectangular duct. The ribs in the V-pattern were tested for both pointing upstream (V-up) and down stream (V-down) to the flow. The angle of inclination of the ribs in inclined and V-pattern was 60°. The enhancement in the Stanton number over the smooth duct was up to 137%, 147%, 134% and 142% for the V-up continuous, V-down continuous, V-up discrete and V-down discrete rib arrangement respectively. The friction factor ratio for these arrangements was up to 3.92, 3.65, 2.47 and 2.58, respectively. Based on the equal pumping power, V-down discrete roughness gave the best heat transfer performance.

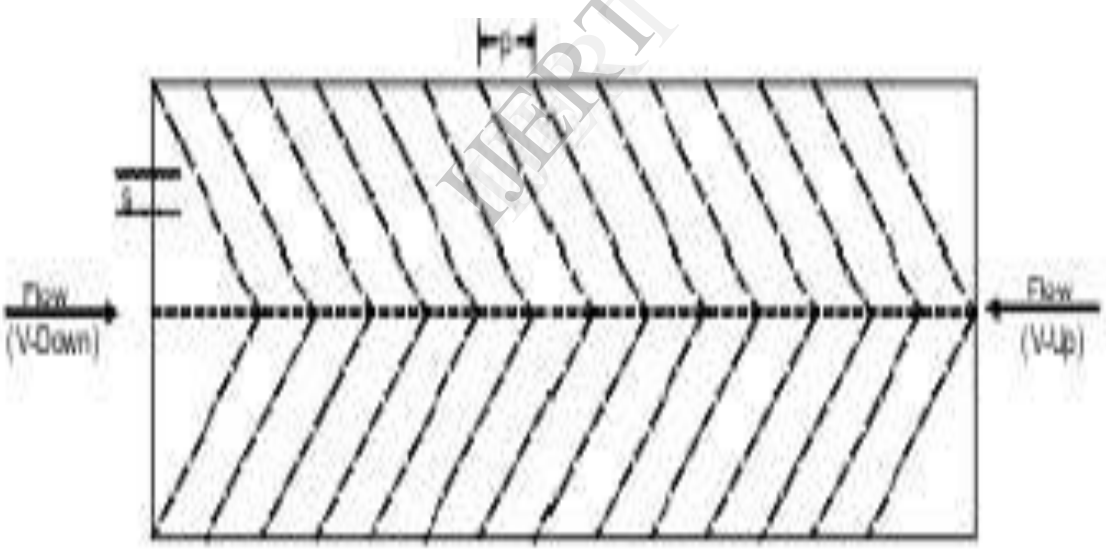

Figure 4: Type and orientation of roughness element investigated by Muluwork *et al.* (1998)

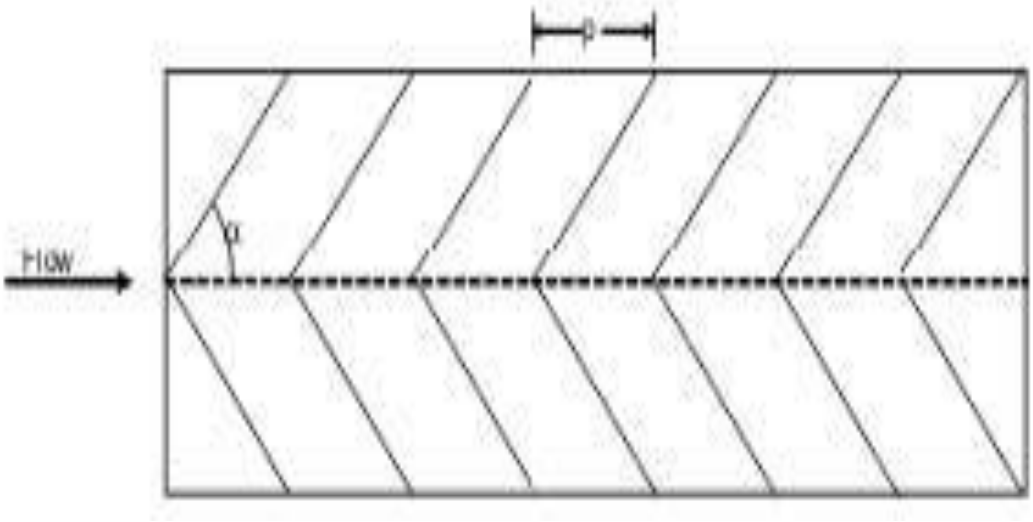

Figure 5: Type and orientation of roughness element investigated by Momin *et al*. (2002)

Broken or discrete rib -Broken V-shaped or broken parallel ribs can create more secondary flow cells and produce more local turbulence in the opposite wall region in comparison to the continuous V-shaped or continuous parallel ribs. The average heat transfer coefficient for the ribbed surfaces turned out to be higher than those for the un ribbed surface by a factor of up to 2 when the transverse ribs were continuous, and by a factor of up to 3 when they were broken. [3] Karwa et al. found that the best heat transfer occurs for the equal pumping power for V-down discrete ribs.[4] Sahu et al. investigated experimentally the effect of pitch varying from 10 to 30 by taking the height of the rib to be 1.5 mm and duct aspect ratio 8 on the heat transfer coefficient and friction factor for 90° broken transverse ribs. It was found that the separation occurred not only at the top edge of the rib but also at the edges at the end of the ribs. This secondary flow interrupted the growth of the boundary layer downstream of the nearby attachment zone in case of 90° broken ribs. It was found out that the maximum Nusselt number attained for a pitch of 20 mm and decreased with an increase in roughness pitch. The maximum thermal efficiency of 83.5 % has been found for a 20 mm pitch. Based on experiments, it was found that the maximum thermal efficiency of a roughened solar air heater was of the order of 51 – 83.5 % depending upon the flow conditions.

[5-6] K.R.Aharwal et al. investigated the effect of gap to width ratio (g/e) and gap to position ratio (d/W) in an inclined split rib arrangement in a rectangular duct of a solar air heater as depicted in Figure 6. A gap in the inclined rib arrangement enhanced the heat transfer and friction factor. The increase in the Nusselt number and friction factor, were in the range of 1.48 to 2.59 times and 2.26 to 2.9 times of the smooth duct, respectively. The maximum values of the Nusselt number, friction factor and thermo-hydraulic performance were observed for a gap in the inclined repeated

ribs with a relative gap position of 0.25 and relative gap width of 1.0.

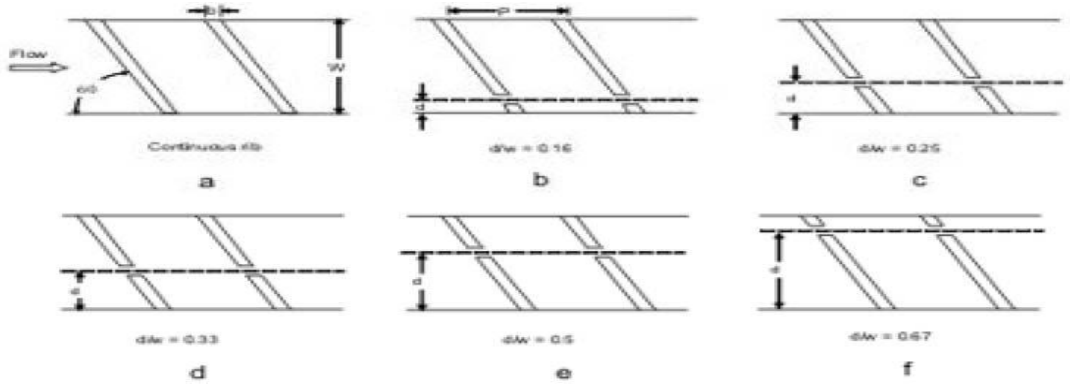

Figure 6: Type and orientation of roughness element investigated by Aharwal *et al.* (2008)

Compound roughness-[7]Eiansa et al. investigated experimentally the combined effect of rib-grooved tabulators on the turbulent forced convection heat transfer and friction characteristics in a rectangular duct. There are three types of rib-groove arrangements: rectangular-rib with triangular-groove, triangular- rib and rectangular-groove and triangular-rib with triangular-groove, which were examined. All rib-groove arrangements significantly enhance the heat transfer rate in comparison with the smooth duct. The thermal enhancement index for the triangular- rib and triangular-groove was achieved and better than that for the rectangular-rib and triangular- groove and triangular-rib and rectangular groove were around 7% and 4% respectively. [8] Jaurker et al. investigated the effect of relative roughness pitch, relative roughness height and relative groove position on a heat transfer coefficient and friction factor of rib-grooved artificial roughness as depicted in Figure 7. The maximum heat transfer was obtained for a relative roughness pitch of about 6, and it was decreased either side of the relative roughness pitch. The optimum condition for heat transfer was found at a groove position to pitch ratio of 0.4 as compared to the smooth duct. As compared to smooth surface, the presence of rib grooved artificial roughness increased the Nusselt number up to 2.7 times, while the friction factor raised up to 3.6 times in the range of parameters investigated.

[9] Layek et al. investigated experimentally the effect of a relative roughness pitch, chamfer angle, relative groove position and relative roughness height on the heat transfer and friction factor for the chamfered rib-groove roughness as depicted in Figure 8. As compared to smooth surface, the chamfer rib-groove roughness resulted in to the increase in the Nusselt number by 3.24 fold and friction factor by 3.78 fold. The maximum heat transfer enhancement occurred for the relative groove pitch of 6 and relative groove position of 0.4. The highest Nusselt number occurred for chamfer angle of 18* but the friction factor increased monotonously with an increase in chamfer angle.[10-11] Varun et al. investigated experimentally the thermal performance of a solar air heater having roughness elements as a combination of

inclined and transverse ribs on the absorber plate as depicted in Figure 9. It was observed that the best thermal performance occurs for a relative roughness pitch (P/e) of 8.

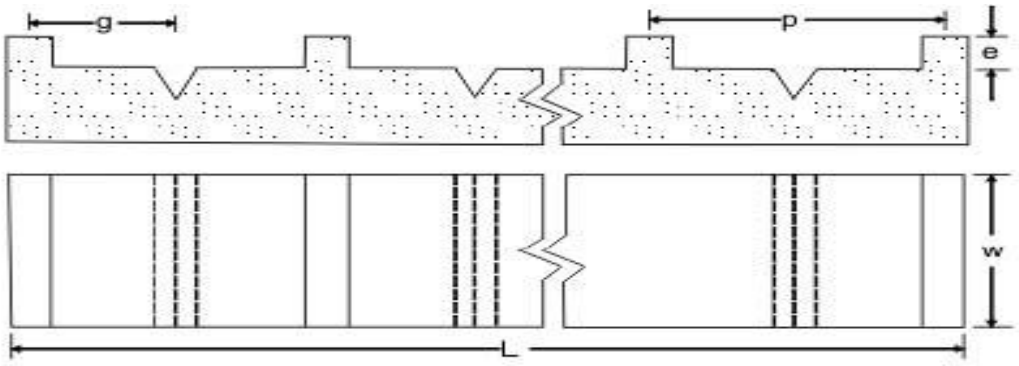

Figure 7: Type and orientation of roughness element investigated by Jaurker *et al.* (2006)

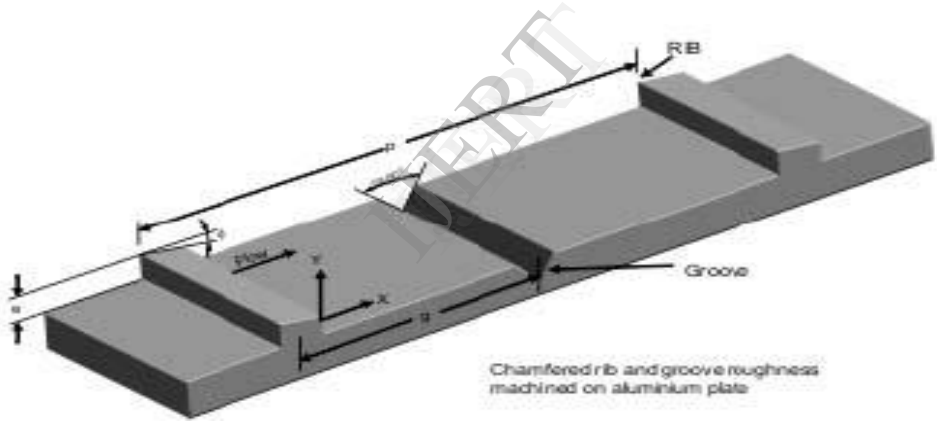

Figure 8: Type and orientation of roughness element investigated by Layek *et al.* (2007)

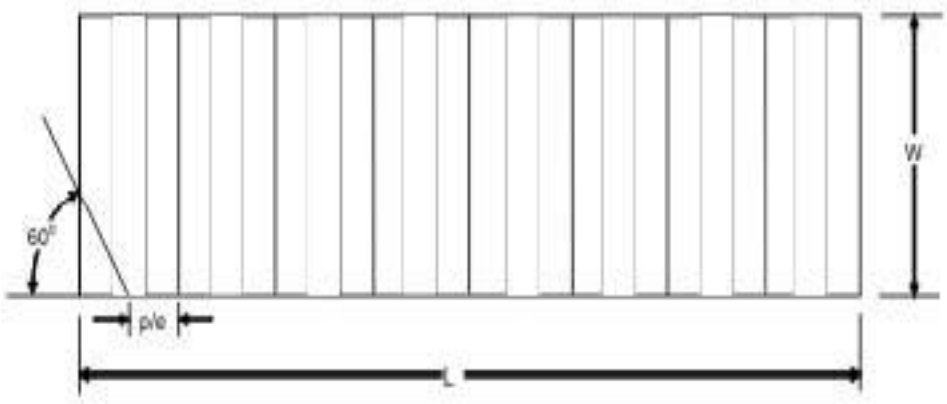

Figure 9: Type and orientation of roughness element investigated by Varun *et al.* (2008)

Small diameter protrusion wires- **[12]**Prasad et al. investigated experimentally the effect of relative roughness pitch (p/e) and relative roughness height (e/D) on the heat transfer coefficient and friction factor of a fully developed turbulent flow in a solar air heater duct with small diameter protrusion wires on the absorber plate. The type and orientation of the geometry is depicted in Figure 10. It observed that the average Nusselt number and as 2.10, 2.24, 2.38 and 3.08, 3.67, 4.25 times that of the smooth duct for relative roughness height of 0.020, 0.027, and 0.033, respectively. It has also been found that increase in the average Nusselt number and average friction factor in the roughened duct were about 2.38, 2.14, 2.01 and 4.25, 3.39, 2.93 times of that of the smooth duct for a relative roughness pitch of 10, 15, and 20, respectively. The maximum enhancement in the heat transfer coefficient and friction factor were as 2.38 and 4.25 times than that of smooth duct respectively.
[13] Gupta et al. investigated the effect of a duct aspect ratio and relative roughness height at a relative roughness pitch of 10, with the Reynolds number range of 3 000 to 18 000, and developed the correlations for heat transfer and friction factor for transverse rib roughness on the absorber plate. It has been found that the behavior of the Stanton number in a transitionally rough flow region was different from its behavior in a fully rough flow region. Correlations for transitionally rough flow regions have been developed for the range of investigation. These correlations showed good agreement between the predicted and experimental values of the heat transfer coefficient and friction factor.
[14] Verma et al. have investigated the effect of similar geometrical parameters of circular wire ribs on heat transfer and friction factor. It was observed that the Nusselt number varied from 1.25 to 2.08 times that of a smooth duct within the range of parameters investigated.

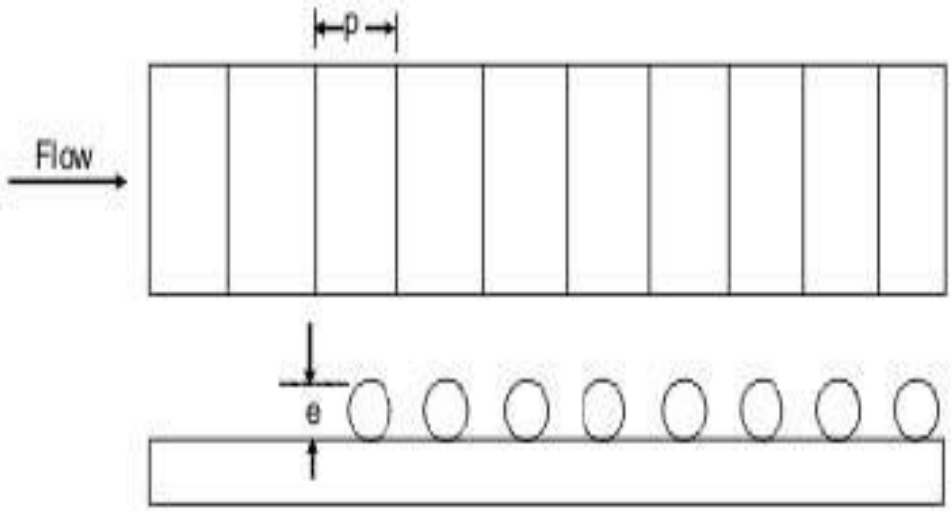

Figure 10: Type and orientation of roughness element investigated by Prasad & Saini (1988)

Expanded wire mesh-[15] Saini et al. investigated experimentally the effect of expanded metal mesh geometry as depicted in Figure 11 for fully developed turbulent

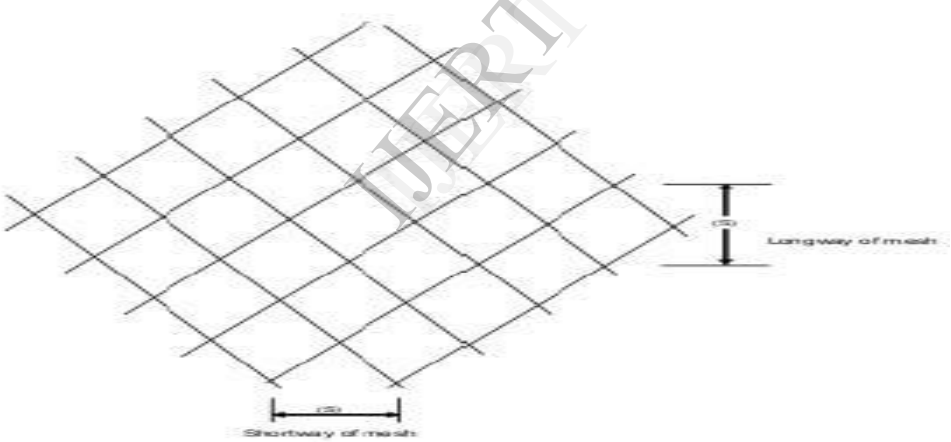

Figure 11: Type and orientation of roughness element investigated by Saini & Saini (1997)

[16-17] Karwa et al. investigated experimentally the effect of repeated chamfered rib-roughness on one broad wall and the duct aspect ratio on the heat transfer coefficient and fluid friction as depicted in Figure 12. It has been observed that the presence of chamfered ribs at one broad wall of the duct yields up to about two-fold and three-fold increase in the Stanton number and the friction factor, respectively, as compared to the smooth duct. The highest heat transfer and also the highest friction factor occur for 15° chamfered ribs. The minima of the heat transfer function occur at a roughness Reynolds number of about 20. The heat transfer function increases with the increase in the aspect ratio from 4.65 to 9.66, and the roughness function decreases

with the increase in the aspect ratio from 4.65 to 7.75. Thereafter, both the functions attain nearly a constant value. There was an appreciable increase in the thermal efficiency (10 to 40 %) of the solar air heaters with chamfered-rib roughened absorber plate due to the enhancement in the Nusselt number of the order of 50 to 120% over the smooth absorber plate. The enhancement in the Nusselt number, friction factor and thermal efficiency were found to be strong functions of the relative roughness height. The greatest enhancement was observed for the air heater with the highest relative roughness height.

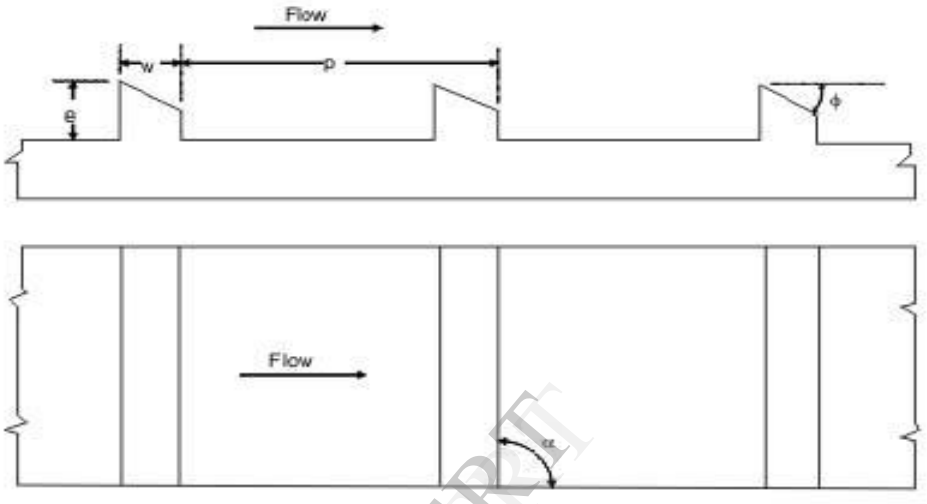

Figure 12: Type and orientation of roughness element investigated by Karwa *et al.* (1999)

Wedge shaped ribs-[18]Bhagoria has performed experiments in order to find out the effect of relative roughness height, relative roughness pitch and wedge angle on the heat transfer and friction factor in a solar air heater roughened duct having wedge shaped rib roughness as depicted in Figure 13.

It has been observed that the maximum heat transfer occurred for a relative roughness pitch of about 7.57, while the friction factor decreased as the relative roughness pitch increased. A maximum enhancement of heat transfer occurred at a wedge angle of about 10°. As compared to the smooth duct, the presence of ribs yielded a Nusselt number up to 2.4 times while the friction factor raised up to 5.3 times for the range of parameters investigated.

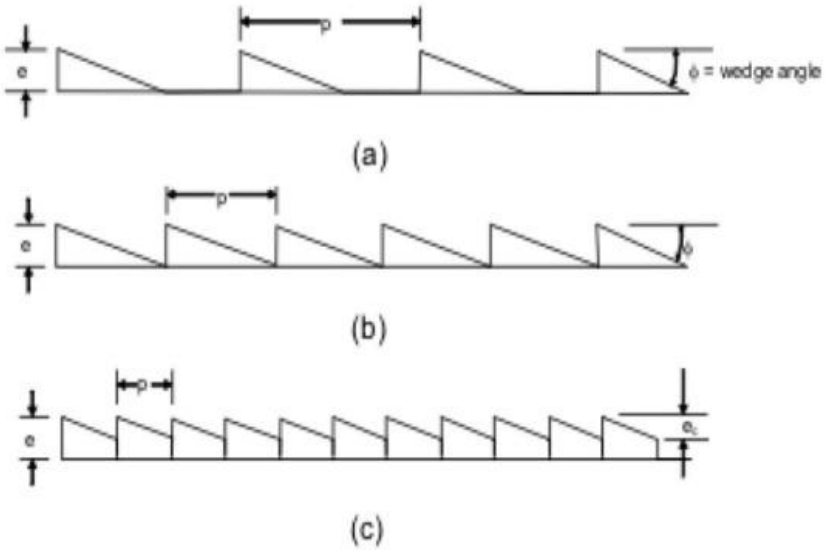

Figure 13: Type and orientation of roughness element investigated by Bhagoria *et al.* (2002)

Arc shaped ribs-[19] Saini et al. investigated experimentally the effect of relative roughness height (e/d) and relative angle of attack (_/90) of arc-shape parallel wire on the heat transfer coefficient and friction factor as depicted in Figure 14 and Figure 15. The maximum enhancement in the Nusselt number was obtained as 3.80 times corresponding to the relative arc angle (_/90) of 0.3333 at relative roughness height of 0.0422. However, the increment in the friction factor corresponding to these parameters was found to be only 1.75 times.

[20]Kumar et al. used Computational Fluid Dynamics for analyzing the performance of a solar air heater duct provided with artificial roughness in the form of thin circular wire in arc shaped geometry. Overall enhancement ratio with a maximum value of 1.7 has been found for the roughness geometry corresponding to the relative arc angle (_/90) of 0.3333 at relative roughness height of 0.0426 for relative roughness pitch of 10. The overall enhancement ratio (OER) given by [21] Wang and Sunden (2002) is as below.

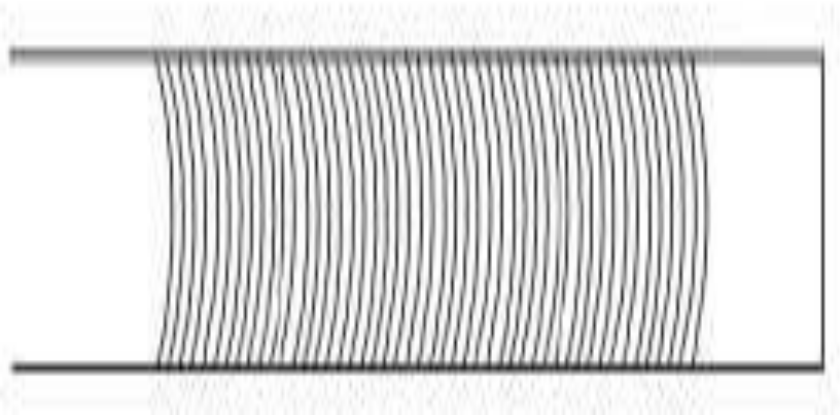

Figure 14: Type and orientation of roughness element investigated by Saini and Saini (2008)

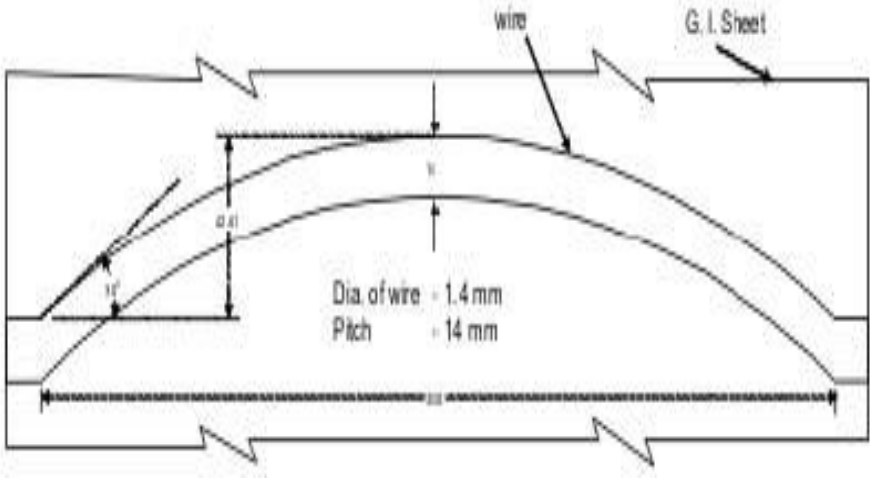

Figure 15: Type and orientation of roughness element investigated by Saini and Saini (2008)

Dimple-[22) Saini et al investigated the effect of relative roughness height (e/D) and relative roughness pitch (P/e) of dimple-shape roughness geometry on heat transfer and friction factor as depicted in Figure 16. It was found that heat transfer could be enhanced considerably as a result of providing dimple- shape roughness geometry on the absorber plate of a solar air heater duct. The maximum value of the Nusselt number was found to correspond to relative roughness height of 0.0379 and relative roughness pitch of 10, while minimum value of the friction factor was found corresponding to relative roughness height of 0.0289 and relative pitch of 10. It was concluded that the roughness parameters of the geometry can be selected by considering the net heat gain and corresponding power required to propel air through the duct

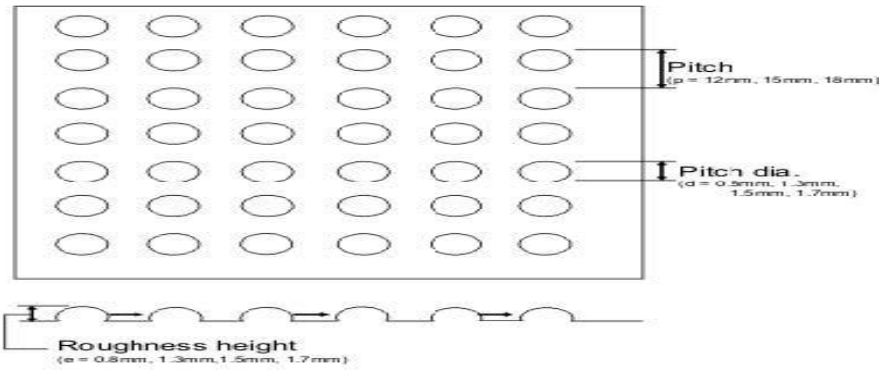

Figure 16: Type and orientation of roughness element investigated by Saini and Verma (2008)

Metal grit ribs-[23] Karmare et al. investigated experimentally the effect of metal ribs of the circular cross section in a staggered manner to form a defined grid as depicted in Figure 17. The effect of the investigated. As compared to a smooth surface, the presence of metal grit ribs on the collector surface of the duct yielded up to two-fold enhancement in the Nusselt number and three-fold enhancement in the friction factor. The highest heat transfer was found for l/s = 1.72, e/D = 0.044 and P/e = 17.5, where the highest friction factor was found for l/s = 1.72, e/D = 0.044 and P/e = 12.5. Optimum performance was observed for l/s = 1.72, e/D = 0.044 and P/e = 17.5 for the range of parameters studied. Enhancement in the Nusselt number was found to be 187% and the friction factor by 213 % as compared with a smooth surface.

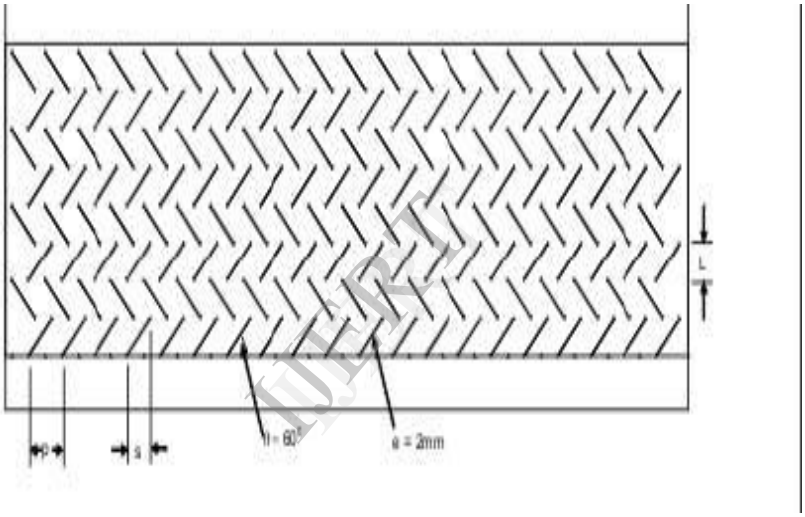

Figure 17: Type and orientation of roughness element investigated by Karmare and Tikekar (2007)

Development of correlation by some artificial roughness geometries used in solar air heater

Roughness geometry	Author	Range of parameters	Correlation	
			Heat transfer coefficient	Friction factor
Transverse small diameter protrusion wire	Prasad and saini	e/D=0.020-0.033 p/e=10-20 Re=50000-50,0000	—	$f_r=2/[0.95(p/e)^{0.53}+2.5\ln(D/2e)-3.75]^2$
Small diameter	Gupta et al.	e/D=0.018-0.052	$Nu=0.0000824(e/D)^{-0.178}$	$f=0.06412(e/D)^{0.019}$

protrusion wire		Re=3000-18,000	$(W/H)^{0.284}(Re)^{1.062}$ e≥35	$(W/H)^{0.0237}$ $(Re^{)-0.185}$
Small diameter protrusion wire	Verma and prasad	e/D=0.01-0.03 p/e=10-40 Re=5000-20,000	$Nu=0.08596(p/e)^{0.054}$ $(e/D)^{0.72}$ $(Re)^{0.723}$ e≤24 $Nu=0.0245$ $(p/e)^{-0.016}(e/D)^{0.21}$ $(Re)^{0.802}$ e≥24	$fr=0.06412(e/D)^{0.019}$ $(W/H)^{0.0237}$ $(Re^{)-0.185}$
V-shaped/inclined wire ribs	Gupta et al.	e/D=0.020-0.053 p/e=7.5-10 $\alpha=30\text{-}60^0$ Re=5000-30,000	$Nu=0.000824$ $(e/D)^{0.178}(W/H)^{0.284\backslash}(Re)^{1.062}$ $\exp[-0.04(1-\alpha/60)^2](k/D)$ e≤35 $Nu=0.00307(e/D)^{0.469}(W/H)^{0.245}$ $(Re)^{0.812}$ $\exp[-0.475(1-\alpha/60)^2](k/D)$ e≥35	$f=.064(e/D)^{0.019}$ $(W/H)^{0.0237}$ $(Re^{)-0.185}$ $^{exp}[-0.0993$ $(1-\alpha/70)^2$]
V-shaped staggered discrete wire ribs	Muluwork et al.	e/D=0.020 B/S=3-9 $\alpha=60^0$ Re=5000-30,000	$Nu_r=0.00534Re^{1.2991}(p/s)^{1.3496}$	$F_r=0.7117$ $(Re^{)2.991}$ $(p/s)^{0.0636}$
V-shaped continuous wire ribs	Momin et al.	e/D=0.020-0.035 p/e=10 $\alpha=30\text{-}90^0$ Re=2500-18,000	$Nu_r=0.067$ $Re^{0.888}(e/D)^{0.424}$ $(\alpha/60)^{-0.077}$ $\exp[-0.0782\{\ln(\alpha/60)\}^2]$ $G=103.77\exp(-0.006)(W/H)^{0.5}(p/e)^{2.56}\exp[0.7343(\ln(p/e))^2]$ $(e+)^{-0.31}$	$F_r=6.266Re^{-0.425}(e/D)^{0.565}$ $(\alpha/60)^{-0.093}$ $\exp[-0.719\{\ln(\alpha/60)\}^2]$
Inclined discrete and continuous wire ribs	Karaw	e/D=0.0467-0.05 p/e=10 $\alpha=60\text{-}90^0$ B/S=3 W/H=7.19-7.75	$G=32.26\exp(-0.006)(W/H)^{0.5}(p/e)^{2.56}\exp[0.7343(\ln(p/e))^2]$ $(e+)^{0.08}$	$R=1.66\exp(-0.0078)(W/H)^{-0.4}(p/e)^{2.695}\exp[-0.762\{\ln(p/e)\}^2$ $(e^+)^{-0.075}]$ for $7\leq e^+\leq20$ $R=1.325\exp(-0.0078)(W/H)^{-0.4}(p/e)^{2.695}\exp[-0.762\{\ln(p/e)\}^2$ $(e^+)^{-0.075}]$ for $20\leq e^+\leq60$

Transverse continuous, Transverse broken and V-shaped broken wire ribs	Tanda	e/H=0.015-0.25 p/e=4.8-13.3 α =40,60 & 90^0 e=3mm, 5mm	$Nu_o=0.023Re_o^{0.8}Pr^{0.4}$ $Re_o=(21.74f\ Re^3)^{0.357}$	$f_0=0.046Re_0^{-0.2}$
Grip shaped wire ribs	Kamare and Tikekar	e/D=0.035-0.044 e/H=12.5-36 I/s=1.72-1 Re=4000-17,000	$Nu=2.4x(Re)^{1.3}x(e/D_h)^{0.42}x(l/s)^{0.146}x(p/e)^{-0.27}$	$f=15.55x(Re)^{-0.26}x(e/D_h)^{0.94}x(l/s)^{-0.27}x(p/e)^{-0.51}$
Gap in inclined continuous wire ribs	Ahawal et al.	e/D=0.0377 p/e=10 W/H=5.87 e&b=2mm d/W=0.167-0.5(4 steps) g/e=0.5-2(4 α =60^0 Re=3000-18,000	$Nu/\ Nu_{r=}$ 2.59	$f/f_s=2.87$
Arc shaped wire ribs	Saini and saini	p/e=10 W/H=12 e/D=0.0123-0.0422 $\alpha/90$=0.333-.0666	$Nu=0.001047Re^{1.3186}x(e/D)^{0.3772}(\alpha/90)^{-0.1198}$	$f=0.14408Re^{-0.17103}x(e/D)^{0.1765}(\alpha/90)^{0.1185}$
Expanded metal mesh	Saini and saini	e/D=0.012-0.0390 L/e=25-71.87 s/e=15.62-46.87	$Nu_r=4x10^{-4}\ Re^{1.22}(e/D)^{0.625}(s/10e)^{2.22}\exp[1.25\{\ln(s/10e)\}^2](l/10e)^{2.66}x\exp[0.824\{\ln(\ l/10e)\}^2]$	$f_r=0.815(Re)^{-0.361}x(l/e)^{0.266}x(s/10e)^{-0.19}x(10e/D)^{0.591}$
Chamfered ribs	Karwal et al.	p/e=4.5-8.5 W/H=4.8,6.1,7.8, 9.66,12 e/D=0.014-0.0320 ϕ= -15,0,5,10,15,18	$G=103.77\exp(-0.006)(W/H)^{0.5}(p/e)^{2.56}\exp[0.7343(\ln(p/e))^2](e+)^{-0.31}$ for $7\leq e^+\leq 20$ $G=32.26\exp(-0.006)(W/H)^{0.5}(p/e)^{2.56}\exp[0.7343(\ln(p/e))^2](e+)^{0.08}$ for $20\leq e^+\leq 60$	$R=1.66\exp(-0.0078)(W/H)^{-0.4}(p/e)^{2.695}\exp[-0.762\{\ln(p/e)\}^2(e^+)^{-0.075}]$ for $7\leq e^+\leq 20$ $R=1.325\exp(-0.0078)(W/H)^{-0.4}(p/e)^{2.695}\exp[-$

				$0.762\{\ln(p/e)\}^2$ $(e^+)^{-0.075}]$ for $20 \leq e^+ \leq 60$
Wedge shaped ribs	Bhagoria et al.	p/e=60.17 W/H=4.8,6.1,7.8, 9.66,12 e/D=0.015-0.033 ϕ= 8,10,12,15 Re=3000-18,000	$Nu_r=1.89x10^{-4}\ Re^{1.22}(e/D)^{0.426}$ $(p/e)^{2.94}$ $\exp[0.71\{\ln(p/e)\}^2](\phi/10)^{-0.018}x\exp[-1.5\{\ln(\phi/10)\}^2]$	$f=12.44(Re)^{-0.18}x(e/D)^{0.99}(p/e)^{-0.52}(\varphi/10)^{0.49}$
Rib groove combination	Jauker et al.	e/D=0.0181-0.0363 g/p=0.3-0.7 Re=3000-21,000 p/e=4.5-10exp[1.513{ln(g/p)^2}+0.8662{ln(g/p)}]	$Nu_r=20.62x10^{-4}\ Re^{0.936}(e/D)^{0.349}$ $(p/e)^{3.318}$ $\exp[.0868\{\ln(p/e)\}^2](g/p)^{1.108}x$ $\exp[2.486\{\ln(g/p)\}^2$ $+1.406\{\ln(g/p)\}]$	$f_r=0.001227(Re)^{-0.199}$ $(e/D)^{0.585}(p/e)^{7.19}$ $\exp[-1.854\{\ln(p/e)\}^2]$ $(g/p)^{0.645}$ $\exp[1.513\{\ln(g/p)\}^2]+$ $0.8662\{\ln(g/p)^3\}$
Chamfered rib groove combination	Layer et al.	e/D=0.022-0.04 p/e=4.5-10 g/p=0.3-0.6 ϕ= 5-3 Re=3000-21,000	$Nu=22.5x10^{-4}\ Re^{0.92}(e/D)^{0.52}$ $(p/e)^{1.72}(g/e)^{-1.21}\ \phi^{1.34}$ $xexp[-0.22\{\ln(\phi)\}^2x$ $xexp[-0.46\{\ln(p/e)\}^2]$ $xexp[-0.74\{\ln(g/p)\}^2]$	$f_r=0.00245(Re)^{-0.124}$ $(e/D)^{0.365}(p/e)^{4.32}$ $(g/p)^{-1.134}$ $Xexp[0.005\phi[exp\{-1.09(lnp/e)^2\}$ $Xexp\ [-0.68(lnp/e)^2]$
Rib dimpled ribs	Saini and verma	e/D=0.018-0.037 p/e=8-12 Re=2000-12,000	$Nu=5.2x10^{-4}\ Re^{1.272}(e/D)^{0.033}$ $(p/e)^{3.15}$ $xexp[-2.21\{\ln(p/e)\}^2x$ $xexp[-1.30\{\ln(e/D)\}^2]$	$f_r=0.0642Re^{-0.423}\ (e/D)^{-0.0214}(p/e)^{-0.465}$ $xexp[0.054\{\ln(p/e)\}^2$ $xexp[0.840\{\ln(e/D)\}^2]$

Relative roughness pitch (p/e)-Various researchers have shown the effect of a relative roughness pitch (p/e) on the flow pattern in Table 1 shows the value of relative roughness pitch (p/e) for a maximum value of a heat transfer coefficient for different types of artificial roughness geometry.

Table 1

Investigators	Roughness geometry	Value of relative roughness pitch (P/e) at which maximum value of heat transfer coefficient
Prasad and Saini (1988)	Wire	10
Karwa et al. (2001)	Chamfered rib	70.9
Bhagoria et al. (2002)	Transverse wedge	7.57
Sahu and Bhagoria (2005)	90°broken transverse	13.33
Jaurker et al. (2006)	Transverse rib-grooved	6
Karmare and Tikekar (2007)	Metal grit rib roughness	17.5
Layek et al. (2007)	Transverse chamfered rib-grooved	6
Varun et al. (2008)	Combination of inclined and transverse ribs	8
Saini and Verma (2008)	Dimple-shape roughness	10

[24] Prasad et al. Figure 1, depicts the flow patterns downstream from a rib as a function of a relative roughness pitch. Due to separation at the rib, reattachment of the free shear layer does not occur for a relative roughness pitch (p/e) – less than about 8 to 10. The maximum heat transfer coefficient occurs in the vicinity of the reattachment point. For relative roughness pitch (p/e) (less than 8 to 10), reattachment will not occur, which results in the decrease of the heat enhancement rate. The rate of increase in the friction factor will increase with the decrease of pitch. However, an increase in the relative roughness pitch (p/e) beyond 10 resulted in the decrease of heat transfer enhancement

.**Figure 1**

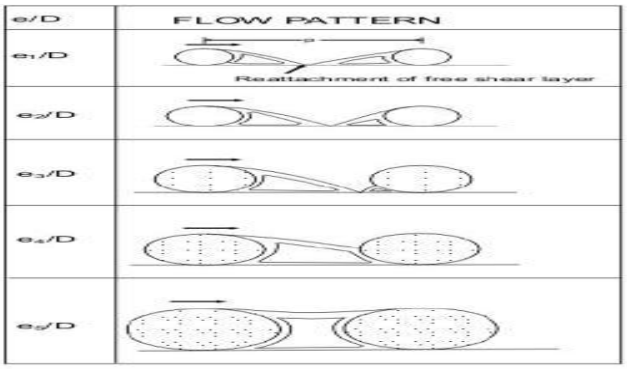

Flow patterns downstream of ribs with the roughness as a function of relative roughness pitch, (Prasad & Saini, 1988)

Relative roughness height (e/D)- [24] Prasad et al. in Table 2 shows the values of the relative roughness height (e/D) for a maximum value of heat transfer coefficient for different roughness geometries used in solar air heater duct.

Table 2

Investigators	Roughness geometry	Value of relative roughness height at which maximum value of heat transfer coefficient
Prasad and Saini (1988)	Wire	0.033
Karwa et al. (2001)	Chamfered rib	0.041
Momin et al. (2002)	V-shaped rib	0.034
Bhagoria et al. (2002)	Transverse wedge	0.033
Jaurker et al. (2006)	Transverse rib-grooved	0.036
Karmare and Tikekar (2007)	Metal grit rib roughness	0.044
Layek et al. (2007)	Transverse chamfered rib-grooved	0.04
Saini and Verma (2008)	Dimple-shape roughness	0.0379
Saini and Saini (2008)	Arc shaped wire	0.0422

[25] Prasad et al. Figure 2, and [25] Prasad et al. Figure 3, depict the flow pattern downstream of a rib and effect on the laminar sub-layer as the rib height is changed respectively. Breakage of the viscous sub layer due to repeated ribs, increases the rate of heat transfer by creating local wall turbulence. If the ribs protrude beyond the viscous sub-layer, they would increase the heat transfer rate, but also cause much higher friction losses. Optimal thermo hydraulic performance conditions are obtained when the roughness height is slightly higher than the transition sub-layer thickness

Figure 2

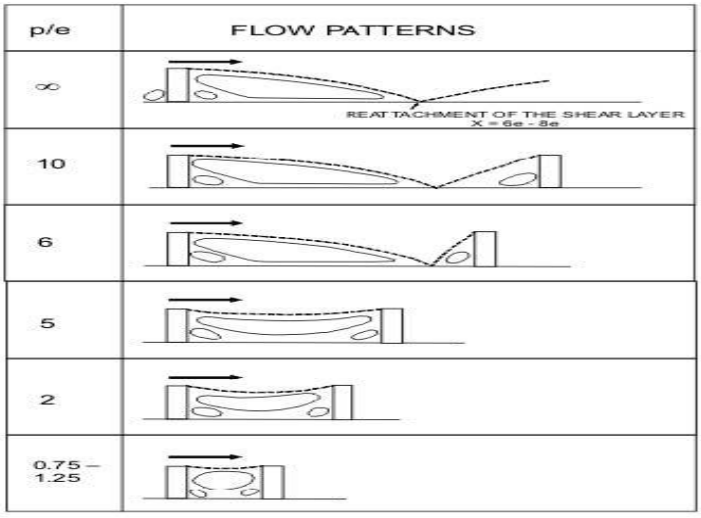

Flow patterns downstream of wires with the roughness as a function of relative roughness height
Source: Prasad & Saini, 1988

Figure 3

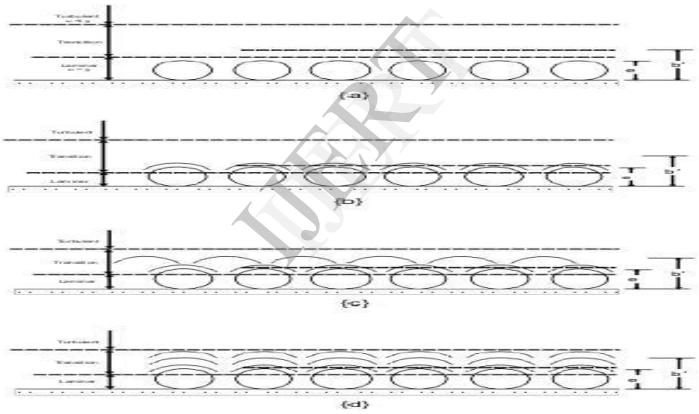

Roughness height with respect to laminar sub layer, Prasad & Saini (1991)

Conclusions

This paper reviews the investigation carried out by various researchers in order to enhance the heat transfer and friction factor by the use of artificial roughness of different shapes, sizes and orientations. It can be concluded that there is a considerable enhancement in heat transfer with little penalty of friction. Correlations developed for heat transfer and friction factor for solar air heater ducts having artificial roughness of different geometries for different investigators are also shown in tabular form. These correlations can be used to predict the thermal efficiency, effective efficiency and then hydraulic performance of artificial roughened solar air heater ducts.

This paper is very helpful for researchers in carrying out the experimental and numerical investigations to find out and optimize the new geometries for the maximum enhancement of heat transfer.

References:-

1. Muluwork, K.B. Saini, J.S. and Solanki, S.C., (1998). Studies on discrete RIB roughened solar air heater, In: Proceedings of National Solar Energy Convention, Roorkee, pp. 75 -84.
2. Momin, A-M E. Saini, J.S. and Solanki, S.C., (2002). Heat transfer and friction in solar air heater duct with V-shaped rib roughness on absorber plate, *Int. Journal of Heat and Mass Transfer*, 45, pp. 3383 – 3396.
3. Karwa, R., (2003). Experimental studies of augmented heat transfer and friction in asymmetrically heated rectangular ducts with ribs on the heated wall in transverse inclined, V-continuous and V-discrete pattern, Int.commn. heat transfer, 30,pp.241-250
4. Sahu, M.M. and Bhagoria, J.L., (2005). Augmentation of heat transfer co-efficient by using 90° broken transverse rib on absorber plate of solar air heater, *Renewable Energy*, 30, pp. 2057 – 2073.
5. Aharwal, K.R. Gandhi, B.K. and Saini, J.S., (2006). Effect of gap in inclined ribs on the performance of artificially roughened solar air heater duct, *Advances in Energy Research*, pp.144-150.
6. Aharwal, K.R. Gandhi, B.K. and Saini, J.S., (2008). Experimental investigation on heat transfer enhancement due to a gap in an inclined continuous rib arrangement in a rectangular duct of solar air heater, Renewable energy, 33, pp. 585 – 596.
7. Eiamsa-ard, S. and Promvonge, P., (2009). Thermal characteristics of turbulent rib-grooved channel flows, Int. Comm. *Heat Mass Transfer*, 36, pp. 705 – 711.
8. Jaurker, A.R. Saini, J.S. and Gandhi, B.K., (2006). Heat transfer and friction characteristics of rectangular solar air heater duct using rib-grooved artificial roughness, *Solar Energy*, 80, pp. 895 – 907.
9. Layek, A. Saini, J.S. and Solanki, S.C., (2007). Heat transfer and friction characteristics for artificially roughened duct with compound turbulators, *International Journal of Heat and Mass Transfer*, 50, pp. 4845 – 4854.
10. Varun, Saini, R.P. and Singal, S.K., (2008). Investigation on thermal performance of solar air heaters having roughness elements as a combination of inclined and transverse ribs on the absorber plate, *Renewable Energy*, 33, pp. 1398 – 1405.
11. Varun, Patnaik, A. Saini, R.P. Singal, S.K. and Siddhartha. (2009). Performance prediction of solar air heater having roughened duct provided with transverse and inclined ribs as artificial roughness
12. Prasad, B.N. and Saini, J.S., (1988). Effect of artificial roughness on heat transfer and friction factor in solar air heater, *Solar Energy*, 41, pp. 555 – 560.

13. *Gupta, D. Solanki, S.C. and Saini, J.S., (1993). Heat and fluid flow in rectangular solar air heater* ducts having transverse rib roughness on absorber plate, *Solar Energy*, 51, pp. 31-37.
14. Verma, S.K. and Prasad, B.N., (2000. Investigation for the optimal thermo hydraulic performance of artificially roughened solar air heaters, *Renewable Energy*, 20, pp.19 – 36.
15. Saini, R.P. and Saini, J.S., (1997) Heat transfer and friction factor correlations for artificially roughened duct with expanded metal mesh as roughness element, *Int. Journal of Heat Mass Transfer*, 40, pp. 973 – 986.
16. Karwa, R. Solanki, S.C. and Saini, J.S., (1999) Heat transfer coefficient and friction factor correlations for the transitional flow regimes in rib-roughened
17. Karwa, R. Solanki, S.C. and Saini, J.S., (2001). Thermohydraulic performance of solar air heaters having integral chamfered rib roughness on absorber plate, *Energy*, 26, pp. 161 – 176.
18. Bhagoria, J.S. Saini, J.S. and Solanki, S.C., (2002). Heat transfer co-efficient and friction factor correlation for rectangular solar air heater duct having transverse wedge shaped rib roughness on the absorber plate, *Renewable Energy*, 25, pp. 341 – 369.
19. Saini, R.P. & Verma, J., (2008). Heat transfer and friction correlations for a duct having dimple shape artificial roughness for solar air heater, *Energy*, 33, pp. 1277- 1287.
20. Kumar, S. and Saini, R.P., (2009). CFD based performance analysis of a solar air heater duct provided with artificial roughness, *Renewable Energy*, 34, pp. 1285 – 1291.
21. Wang, L. and Sunden, B., (2002). Performance comparison of some tube inserts, *Int. Comm. Heat Mass Transfer*, 29, pp. 45 – 56.
22. Saini, S.K. and Saini, R.P., (2008). Development of correlations for Nusselt number and friction factor for solar air heater with roughened duct having arcshaped wire as artificial roughness, *Solar Energy*, 82, pp. 1118 – 1130.
23. Karmare, S.V. and Tikekar, A.N., (2007). Heat transfer and friction factor correlation for artificially roughened duct with metal grit ribs, *Int. Journal of Heat Mass Transfer*, 50, pp. 4342 –4351.
24. B.N. Prasad, and J.S. Saini, Effect of artificial roughness on heat transfer and friction factor in solar air heater, Solar Energy, 41, pp. 555–560. (1988).
25. Prasad, B.N. and Saini, J.S., (1991). Optimal thermo hydraulic performance of artificial roughness solar air heater, Solar Energy, 47, pp 91 – 96.